Microchimica Acta (2019) 186: 54
https://doi.org/10.1007/s00604-018-3117-7

ORIGINAL PAPER

Voltammetric determination of caffeic acid by using a glassy carbon electrode modified with a chitosan-protected nanohybrid composed of carbon black and reduced graphene oxide

Kannaiyan Pandian[1] · Dhamodaran Mohana Soundari[1] · Panneerselvam Rudra Showdri[1] · Jayaprakash Kalaiyarasi[1] · Subash C. B. Gopinath[2,3]

Received: 1 November 2018 / Accepted: 25 November 2018 / Published online: 7 January 2019

Abstract
Differential pulse voltammetry (DPV) was employed for the determination of caffeic acid (CA) in acidic solutions by using a glassy carbon electrode (GCE) modified with a chitosan-protected nanohybrid composed of carbon black and reduced graphene oxide. Electrochemical impedance spectroscopy and cyclic voltammetry were utilized to study the interfacial electron transfer on the modified GCE. Cyclic voltammetry shows that CA exhibits a reversible redox reaction with an oxidation peak at + 0.30 V (vs. Ag/AgCl) and a reduction peak at + 0.24 V in pH 3.0 solution at a scan rate of 50 $mV \cdot s^{-1}$. Under the optimized experimental conditions, the response to CA is linear in 0.3×10^{-9} to 57.3×10^{-5} M concentration range. The limit of detection is 0.03×10^{-9} M (at an S/N ratio of 3), and the electrochemical sensitivity is 5.96 $\mu A \cdot \mu M^{-1} \cdot cm^{-2}$. This sensor for CA displays better sensitivity and a response over a wider concentration range. It was applied to the determination of CA at trace levels in various (spiked) wine samples.

Keywords Electrochemical sensor · Electrode preparation · Interference of polyphenols · Amperometry method · Wine samples

Introduction

Caffeic acid (3,4-dihydroxycinnamic acid) (CA), a phenolic acid is present in fruits, grains, vegetables, wines, and coffee [1–4]. CA is widely revealed in the areas of biochemistry and medicine mostly the biological aspects including anti-inflammatory, anticancer, antipruritic, anticarcinogenic, immune regulator, which have enthused the researchers to aim on the electrochemical detection of caffeic acid [5–8]. Different analytical techniques have been developed to determine the CA, including capillary electrophoresis [9], Gas Chromatography-Mass Spectroscopy [GC-MS] [10], flow injection system [11], and voltammetric method [12]. These above methods need sophisticated facilities, highly skilled technicians for operating this instruments and time-consuming process. Among all these methods, the electrochemical methods are more favoured due to exceptional sensitivity, low cost, good selectivity, reliability, and its simplicity. Some of the polymers like chitosan (Chit), pectin, alginate and cellulose acetate have been widely utilized for the modified surface with the electrochemical analysis of the target in the occurrence of other interfering compounds even in larger extent. In particular, chitosan is a biodegradable polysaccharide and non-toxic [13] and is utilized in gene delivery [14], food sector [15], and

Electronic supplementary material The online version of this article (https://doi.org/10.1007/s00604-018-3117-7) contains supplementary material, which is available to authorized users.

✉ Kannaiyan Pandian
jeevapandian@yahoo.co.uk

Dhamodaran Mohana Soundari
dmohana7@gmail.com

Panneerselvam Rudra Showdri
roudrashowdri@gmai.com

Jayaprakash Kalaiyarasi
kalaiyarasijayaprakash@yahoo.com

Subash C. B. Gopinath
subash@unimap.edu.my

[1] Department of Inorganic Chemistry, University of Madras, Guindy Campus, Chennai 600 025, India

[2] Institute of Nano Electronic Engineering, Universiti of Malaysia Perlis, 01000 Kangar, Perlis, Malaysia

[3] School of Bioprocess Engineering, Universiti of Malaysia Perlis, 02600 Arau, Perlis, Malaysia

tissue engineering [16]. Further, the use of chitosan is to improve the stability of nanomaterials and electrodes [17–19]. Graphene oxide (GO) has enormous attraction due to its outstanding properties like high elasticity, quantum electronic transport and high mobility [20]. Because of its high thermal stability, electronic conductivity and excellent film-forming properties, rGO has been utilized for the fabrication of electrodes [21, 22]. Carbon black (CB) is an amorphous carbon material which is made up of sp^2 hybridized carbon atoms and few sp^3 carbon atoms. Filho et al., demonstrated the electrochemical sensor based on rGO/CB/chitosan in which glutaraldehyde was used as cross-linker for simultaneous analysis of dopamine and paracetamol in urine samples [23].

We demonstrate a novel biosensor using chitosan protected carbon black and rGO hybrid layer on GCE. In CV technique, the modified electrode compared with the bare GCE, the Chit-rGO/CB/GCE provides improved redox peak currents and decreased over potential value. The results of the present analysis were compared to high-performance liquid chromatography (HPLC). The fabricated electrode displayed good reproducibility and sensitivity with wide linear range, long-term storage stability and practical feasibility for the quantitative electrochemical detection of CA in different wine samples.

Experimental

Reagents and apparatus

Natural graphite flakes, 3,4-dihydroxycinnamic acid, chitosan, potassium ferricyanide [$K_3(Fe(CN)_6$] were procured from Sigma-Aldrich (Biocorporals Pvt. Ltd., Chennai, India, www.biocorporals.net). Potassium chloride (KCl), potassium dihydrogen phosphate (KH_2PO_4), potassium hydrogen phosphate (K_2HPO_4), potassium nitrite (KNO_3), dimethyl sulfoxide (DMSO), hydrogen peroxide (H_2O_2), acetic acid (CH_3COOH), hydrochloric acid (HCl), ethanol (C_2H_5OH), and potassium permanganate ($KMnO_4$) were received from SRL Pvt. Ltd. (Vijaya Scientific, Chennai, India, www.vijayascientific.com). All reagents were of analytical grade and used directly. A buffer (pH 3.0) was made by mixing 0.1 M KCl, 0.1 M KH_2PO_4, and 0.1 M K_2HPO_4 in 250 mL of doubly distilled water. The stock solution of 0.1 M caffeic acid was prepared by double distilled water and kept at 5 °C.

Electrochemical impedance spectroscopy (EIS) analyses were performed utilizing the CHI-660B electrochemical system by applying AC voltage of 5 mV amplitude at the desired frequency ranges (from 0.01 Hz to 100 kHz). The electrolyte was made by using 10 mM $[Fe(CN)_6]^{3-/4-}$ containing 0.1 M KNO_3 in 100 mL standard flask utilizing double distilled water as a redox probe.

Morphological observations were carried out by field emission scanning electron microscopy (FE-SEM, SU6600, and Hitachi, Japan) at an operating voltage of 15 kV. Fourier transform infrared (FT-IR) spectra were observed by a Perkin-Elmer 190 FT-IR spectrometer with a resolution of 4 cm^{-1} for 32 scans over wave number ranges of 4000–400 cm^{-1}. Atomic force microscopy (AFM) images were recorded by AFM park systems (XE-70, South Korea). The electrochemical analysis was carried out using CHI 660B electrochemical instrument (Texas, USA). A single compartment electrochemical cell with 3 electrode systems containing GCE (of 3 mm diameter), platinum wire (of 0.5 mm diameter) and Ag/AgCl (3.0 M KCl) was utilized as working, counter and reference electrodes, respectively. Bioanalytical system polishing kit was used as received from BAS instruments (USA) to polish the GCE surface.

The modified electrode was detected utilizing cyclic voltammetry (Potential window: + 0 V to +0.7 V, Scan rate: 50 $mV.s^{-1}$), chronoamperometric curve of CA oxidation was observed at a polarization voltage of +0.3 V, differential pulse voltammetry (Scan rate: 0.02 $V.s^{-1}$, pulse width: 0.05 s, pulse amplitude: 0.025 V) and amperometric (i-t) curves of CA were observed at an applied potential of +0.3 V under hydrodynamic conditions.

The preparation procedure of graphene oxide (by Hummers' method) and synthesis of Chit-CB/rGO nanocomposites are discussed in Electronic Supporting Information (ESM). In the present system, we prepared a reduced graphene oxide by thermal annealing of graphite oxide [24] and the nanocomposites to obtain a stable thin film as a surface modifier as well as electron transfer mediator.

Electrode preparation

The Chit-CB/rGO nanocomposites modified GCE was made-up by the following procedure: The electrode surface was first mechanically polished with alumina (0.05 μm powder) paste and thoroughly rinsed extensively with double distilled water and then washed by nitric acid and ethanol (1:1 *v/v*). Eventually, the electrode was rinsed with ethanol in the ultrasonic bath for 45 min to get a mirror-like surface and dried at room temperature. About, 2 mg of Chit-CB/rGO nanocomposites was dispersed in 2 mL of ethanol and sonicated for 10 min to get a homogeneous dispersion of nanocomposites. The colloidal suspension of Chit-CB/rGO (5 μL) was dropped cast onto the GCE surface and dried at room temperature for overnight.

Results and discussion

Choice of materials

Reduced graphene oxide has a higher surface area than graphite powder and also graphene has higher conductivity. Also, it is easy to prepare a nanocomposite by dispersing a known amount of rGO into the chitosan solution. By this way we can prepare a stable thin film of the graphene-modified electrode. Moreover, the reduced graphene oxide possess exceptional features such as high electrical conductivity, high mechanical stability, large surface area (2630 m^2 g^{-1}), and highly resistant against electrochemical corrosion when it is investigated in aqueous electrolytes. Thus, rGO is considered highly efficient and potential material for electrochemical applications. Hence, we chose rGO as one of the electrode material for electrochemical sensing of various analytes.

Morphological studies of chit-CB/rGO nanostructures

Characterized the Chit-CB/rGO hybrid nanocomposites by FT-IR, SEM and AFM techniques. The structural and morphology of Chit-CB/rGO nanocomposite was measured by FE-SEM studies. Figure 1a, displays the layered structured sheet-like morphology features of rGO, which consisted of wrinkles and folding. The layered structure of graphene is also seen clearly in Fig. 1b, with individual carbon black particles firmly form a stable film on the rGO sheet (indicated in yellow dotted circles). The composition of elements in rGO was estimated by energy dispersive X-ray analysis (EDAX) (Fig. S1). The EDAX spectra of the rGO sheets contained the occurrence of an atomic carbon (92.68%) and oxygen (7.32%). The nanostructures graphene sheets possess layered structure, which aids a large area and excellent electrochemical responses.

Furthermore, Atomic force microscopy (AFM) image was observed for Chit-CB/rGO, the same trend was noticed like FE-SEM observations (Fig. S2). The roughness of the carbon particle was noticed to be 40 nm. The averaged roughness of the Chit-CB/rGO surface was found to be 40 nm which was estimated from AFM studies.

FI-IR studies

The nature of bonding between chitosan and carbon black modified graphene sheet was confirmed by FT-IR spectra. The infrared spectra of a) Chitosan, b) rGO, and c) Chit-CB/rGO were shown in Fig. S3. In Chit-CB/rGO nanocomposites, a broad and strong absorption band at 3350 cm^{-1} was observed owing to O-H vibration stretching [25]. The C=O stretching vibration of carboxyl groups situated at edges of the graphene layer is noted at 1764 cm^{-1}. The absorption band at 1595 cm^{-1} (ν_{CO-NH}) is indicating the covalent modification of carbon black and chitosan which confirms the formation of Chit-CB/rGO nanocomposites [26].

EIS studies

A Nyquist plot displaying a model circuit for electron transfer resistance (R_{ct}), and the element of Warburg impedance (W) shown the real $[Fe(CN)_6]^{3-/4-}$ electron transfer of the redox probe and its fitted values for all electrodes were given in the Table. S1 (ESI). In this study, the AC signal amplitude of 5 mV over a frequency at 0.01 Hz to 100 kHz with 10 mM $[Fe(CN)_6]^{3-/4-}$ containing 0.1 M KNO_3 as a redox probe. The a) bare/GCE, b) rGO/GCE, and c) Chit-CB/rGO/GCE exhibited electron transfer resistance values of 148 Ω, 137.2 Ω, and 103.5 Ω, respectively as shown in Fig. 2a. This indicates that the $[Fe(CN)_6]^{3-/4-}$ as a redox probe have facile electron transfer kinetics at the Chit-CB/rGO/GCE. This is might be due to the rapid charger transfer of Chit-CB/rGO/GCE nanocomposites, which results in an improved electron transfer rate of the electrode surface and facilitate the electron transfer between the surface of the electrode and redox probe. These excellent electrochemical characteristics of Chit-CB/rGO/GCE are beneficial for the practical utilities.

Electrochemical characterization of chit-CB/rGO/GCE

The electrochemical properties of the different modified electrodes were investigated by CV technique. From the Fig. 2b, shows the cyclic voltammograms of 10 mM $K_3[Fe(CN)_6]^{3-/4-}$ containing 0.1 M KNO_3 as a redox probe at a scan rate of 50 $mV.s^{-1}$ with a) bare/GCE, b) rGO/GCE, and c) Chit-CB/rGO/GCE. It was seen that a pair of redox peaks with the

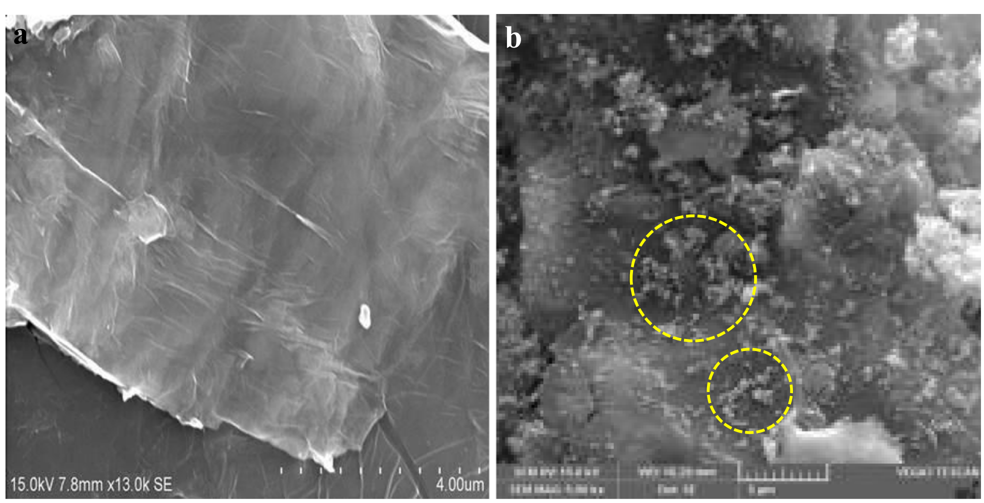

Fig. 1 FE-SEM micrographs of **a**) rGO, **b**) Chit-CB/rGO nanocomposites (yellow dotted circles indicate individual carbon black particles on the rGO sheet)

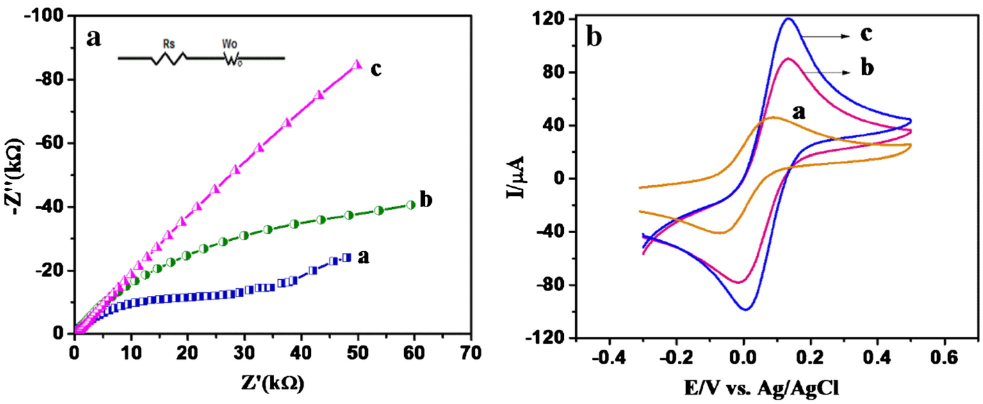

Fig. 2 Nyquist plots of **a**) bare GCE, **b**) rGO/GCE, and c) Chit-CB/rGO/GCE in the presence of 10 mM $[Fe(CN)_6]^{3-/4-}$ containing 0.1 M KNO_3 as the supporting electrolyte. AC Amplitude: 5 mV; Frequency range: 0.01 Hz to 100 kHz. Inset: Randles equivalent circuit (A). CV behavior of **a**) bare GCE, **b**) rGO/GCE, and **c**) Chit-CB/rGO/GCE in the presence of 10 mM $[Fe(CN)_6]^{3-/4-}$ containing 0.1 M KNO_3 solution, recorded at a scan rate of 50 $mV{\cdot}s^{-1}$ (B)

anodic peak to cathodic peak separation of potential, ($\Delta Ep = E_{anodic\ peak} - E_{cathodic\ peak}$) ΔEp of 125 mV appears for bare GCE (curve a) whereas in rGO/GCE, the redox peak currents slightly increase and the peak separation value of $\Delta Ep =$ 115 mV, indicating that the electrochemical reaction of the $[Fe(CN)_6]^{3-/4-}$ probes at the rGO/GCE (curve b) is quasi-reversible and undergoes sluggish electron transfer process of kinetic. This is primarily attributed to the poor electrical conductivity of rGO. But Chit-CB/rGO/GCE shows a good resolved redox peak of anodic and cathodic peak potentials, + 0.130 V and + 0.058 V (vs. Ag/AgCl), respectively. The peak separation potential value between anodic peak potential and cathodic potential ($\Delta E_p = E_{pa} - E_{pc}$) was found to be 72 mV at 50 $mV{\cdot}s^{-1}$ and a redox peak current ratio are about one ($I_{pa}/I_{pc} \approx 1$), which shows reversible and one-electron transfer process of the electrochemical reaction. The Chit-CB/rGO/GCE yield the maximum peak current among all other different electrodes, possibly because of the accelerated $[Fe(CN)_6]^{3-/4-}$ diffusion towards the surface by a layer of graphene.

Obviously, the Chit-CB/rGO/GCE nanomaterials exhibited much higher electrocatalytic activity, increased electroactive surface area, and faster electron-transfer kinetics (reflected in the lower peak to peak separation) compared to the modified electrode including bare GCE.

To calculate the electro-active surface area (A) of the CB/rGO/GCE and Chit-CB/rGO/GCE the Randles-Sevcik equation was used in which assume the mass transport is taken place only by the diffusion process [27]:

$$I_p = 2.69 \times 10^5 A\, D^{1/2}\, n^{3/2}\, \upsilon^{1/2}\, C \qquad (1)$$

Here, *n* represents the number of electrons connecting in the redox behavior, *D* indicates the diffusion coefficient of the $K_3[Fe(CN)_6]^{3-/4-}$ (equal to 6.37×10^{-6} cm^2/s), *C* represents the bulk of the redox probe ($mol{\cdot}cm^{-3}$), and υ represents the scan rate ($mV{\cdot}s^{-1}$). The electro-active surface area of CB/rGO/GCE and Chit-CB/rGO/GCE were estimated as 0.73×10^{-4} cm^2 and 1.19×10^{-4} cm^2. It is attractive to indicate that the modified electrode of Chit-CB/rGO/GCE has increased surface area and highly active against the CB/rGO/GCE electrode and also the oxidation peak current is highly superior. This indicates that the Chit-CB/rGO/GCE might be very active in electrochemical detection of different biomolecules and drugs.

Electrochemical behaviour of CA at the chit-CB/rGO/GCE

In order to study the electrocatalytic oxidation of CA at Chit-CB/rGO/GCE nanocomposite, we investigated the cyclic voltammogram response of a) and b) bare GCE in absence and presence of 2.6×10^{-4} M of CA, and c) Chit-CB/rGO/GCE in the presence of 2.6×10^{-4} M of CA with buffer (pH 3.0) at a desired scan rate (50 $mV{\cdot}s^{-1}$). As shown in Fig. 3, in bare GCE, a poor redox peak was noticed with an

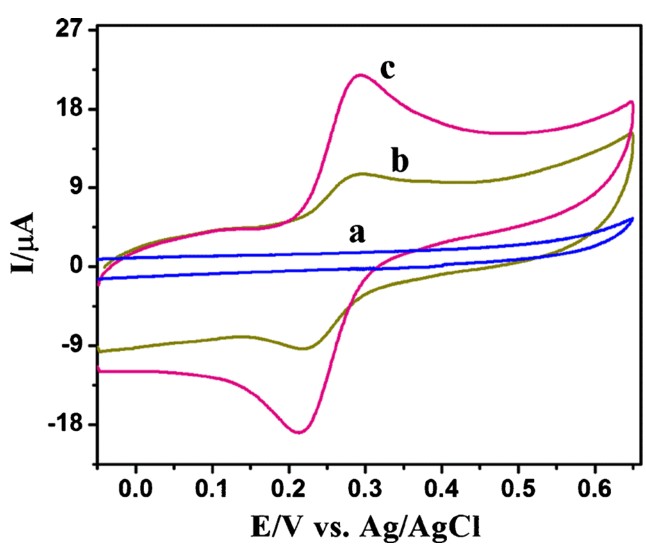

Fig. 3 Cyclic voltammograms of **a**) bare/GCE, **b**) 2.6×10^{-4} M of CA on GCE, and **c**) Chit-CB/rGO/GCE in the presence of 2.6×10^{-4} M of CA with 0.1 M buffer (pH 3.0) at a scan rate of 50 $mV{\cdot}s^{-1}$

oxidation peak potential + 0.290 V vs. Ag/AgCl, respectively, whereas in Chit-CB/rGO/GCE a minor shifting with the peak of + 0.3 V was observed. Chit-CB/rGO/GCE shows redox peaks for CA with a peak-to-peak separation value of Δ_{Ep} = 60 mV (E_{pa} - E_{pc} = 0.300 V – 0.240 V), which is lower than bare GCE. Finally, Chit-CB/rGO/GCE shows a well-defined pair of redox peak for CA, representing the electrochemical redox process of CA is reversible. Further, the anodic peak current signal of CA at the Chit-CB/rGO/GCE was three times more than the bare GCE. The redox peak current values increase with an increase the CA and a linear relationship was recognized from the CA from 1.3× 10^{-4} to 12.7× 10^{-3} M as shown in Fig. S4 (A). The linear regression equation is: I_{pa} = 9.5590 C (mM) – 5.4274, I_{pc} = −6.7467 C (mM) + 3.9531 with correlation coefficient R^2 as 0.9992 and 0.9994 as displayed in Fig. S4 (B). The above results indicate that the nanocomposites highly enhanced electron transfer rate, owing to its unique physicochemical characteristics (the sheets like structure, large surface area, high conductivity, etc).

Optimization of method

The following parameters like scan rate (a), buffer pH value (b) were experimentally shown and the corresponding data and figures are displayed (Fig. S5 and Fig. S6). The influence of the scan rate and the pH of the medium on electrochemical oxidation of caffeic acid were investigated. The maximum current response and most favourable pH of the electrochemical oxidation were derived from graphical values [Optimum buffer pH = 3.0 (a), and the scan rate: 50 mV·s^{-1} (b)]. The electron transfer coefficient (α) and the number of electron transfer (n) were found to be 0.60 and 2.0 [the results are shown in Electronic Supporting Information (ESI)].

Chronoamperometry studies

Chronoamperometry analysis was performed to recognize the diffusion coefficient of CA oxidative at Chit-CB/rGO/GCE. Fig. S7A, displayed the current-time relationships of Chit-CB/rGO/GCE were achieved by the working electrode potential of +0.30 V (vs. Ag/AgCl) for CA at different concentrations of 0.6 × 10^{-6} M to 3.3 × 10^{-6} M in presence of 0.1 M buffer (pH 3.0). To estimate, the diffusion coefficient (D) of Chit-CB/rGO, the linear plot of I_p versus $t^{-1/2}$ was attained by comparing a) to e) that results in straight lines (Fig. S7B). The plot of slope vs.conc. of CA (mM) is displayed in Fig. S7C.

The diffusion coefficient (D) and catalytic rate constant (k_h) value of caffeic acid were found to be 1.06 × 10^{-6} $cm^2 \cdot s^{-1}$ and 6.7 × 10^6 $cm^3 \cdot mol^{-1} \cdot s^{-1}$ at Chit-CB/rGO/GCE, which are discussed in the Supporting Information (ESI).

Differential pulse voltammetry

To explore the analytical characteristics of the optimized Chit-CB/rGO/GCE for the detection of CA. Fig 4a, displays the differential pulse voltammograms of the modified electrode in 0.1 M buffer (pH 3.0) having CA. The oxidation peak current (I_p) was enhanced with enhancing concentration of CA from 0.6 × 10^{-6} M to 10.6 × 10^{-5} M. The regression calibration plot was made from I_{pa} vs. Conc. of CA with the correlation coefficient estimated as (R^2 = 0.9967) as shown in Fig. 4b. The current sensitivity was found to be 2.1460 μA·mM^{-1}·cm^{-2}. Thus, the detection limit and quantification limit have been estimated using the standard equation: LOD = 3σ/slope and LOQ = 10σ/slope (where σ = standard deviation of the blank signal). As a result, the LOD and LOQ are noticed to be 0.021 × 10^{-6} M and 0.072 × 10^{-6} M, respectively. A stable and sharp electrochemical behaviour of Chit-CB/rGO towards the sensing of CA at it's a great electrocatalytic activity and it is owing to the synergistic effects of the stacked CB/rGO sheets and homogeneously embedded chitosan film.

Amperometric (i-t) determination of CA

The electrochemical analysis of CA at Chit-CB/rGO modified GCE was done by amperometric (i-t) technique with the used potential of + 0.3 V under hydrodynamic conditions. The resulting (i-t) graph is shown in Fig. 4c. A quick and steady electrochemical response was noted for each addition of CA. The oxidation peak current enhances with enhancing the CA concentration. The amperometric current signal was found to enhance linearly in the concentration range of 0.3 × 10^{-9} M to 57.3 × 10^{-5} M for CA as shown in Fig. 4d. The linear regression equation as: Ip (μA) = 0.1973 C (μM) + 0.1322 with a correlation coefficient (R^2) of 0.9990, respectively, which proves the better relationship between I_{pa} vs. Conc. of CA. The detection limit and LOQ was calculated in the graph of CA and it was found to be 0.03 × 10^{-9} M and 0.039 × 10^{-9} M based on the ratio of signal-to-noise with a current sensitivity of 5.9602 μA·μM^{-1}·cm^{-2}. The electrocatalytic activity of Chit-CB/rGO/GCE is because of the hybrid structural effect of carbon back and reduced graphene oxide with the large surface area, which provides catalytic active sites for the CA estimation. The electrochemical behaviour of Chit-CB/rGO/GCE was quite comparable with the previously revealed CA sensors with the estimated analytical parameters namely concentration ranges, current sensitivity, and the detection limit (Table 1). The results confirmed evidently that the Chit-CB/rGO/GCE might be utilized for the determination of CA in low concentration with enhanced current sensitivity and rapid signal.

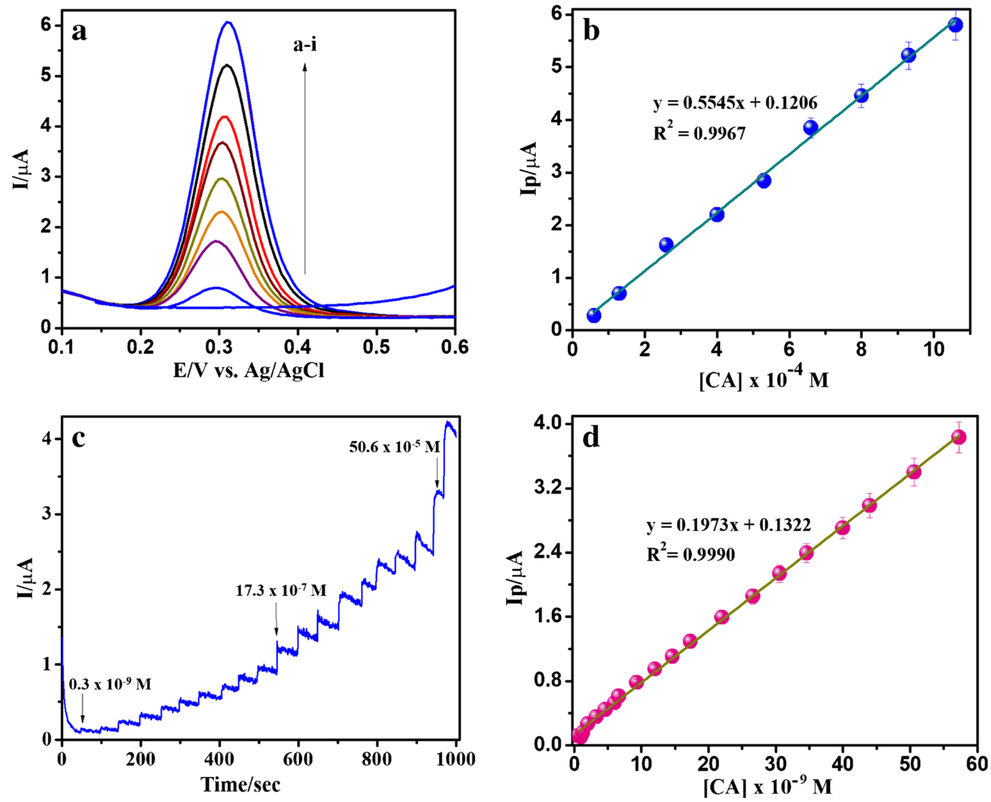

Fig. 4 DPV of Chit-CB/rGO modified GCE in different concentrations of 0.6×10^{-6} M to 10.6×10^{-5} M of CA in 0.1 M buffer (pH 3.0) (**a**). Calibration plot of I_{pa} vs. Conc. of CA (**b**). Amperometric response of Chit-CB/rGO modified GCE at an used potential 300 mV to subsequent addition with concentrations from of 0.3×10^{-9} M to 57.3×10^{-5} M of CA in the occurrence of in 0.1 M buffer (pH 3.0) (**c**). Calibration plot I_{pa} vs. Conc. CA (D)

Interference studies

The selectivity of the modified electrode is significantly improved for the voltammetry recognition of CA. Therefore, we studied the selectivity of Chit-CB/rGO/GCE nanocomposites in the occurrence of potentially active interfering species by using amperometry method (Fig. 5). As a result, shows that 1000-fold raise in concentration of redox active substance like polyphenols, flavonoids such as eugenol, ellagic acid, chlorogenic acid, quercetin, and gallic acid, are slightly increase of the current signal in the case of polyphenols and quercetin which means that the inference of other polyphenols and flavanoid interference is negligible one (Fig. 5). For instant 1 µM of CA current response is equal to 13 mM of flavonoids and polyphenols showing that the modified electrode as selective for CA quantitation. On the other hand, 1000-fold raise in the concentration of Zn^{2+}, KCl, NaCl, Mg^{2+}, cinnamic acid, and Ca^{2+}, do not shows any influence in current signal and other similar redox molecules include ascorbic acid, dopamine, uric acid and paracetamol species are shows a poor current responses in the low concentration ranges of CA. Furthermore, we also investigated the influences of 300- fold concentration of some saccharides and pollutants like glucose, fructose, hydrazine, and nitrite does not disturb the current signal of CA. From the interference studies it is observed that the detection of CA can be performed by applying a constant voltage of + 0.30 V vs. Ag/AgCl under the constant stirring condition for the real sample analysis.

Reproducibility and stability

To investigate the repeatability, five different Chit-CB/rGO modified GCE at 2.6×10^{-6} M of CA were subjected to DPV in the occurrence of 0.1 M buffer (pH 3.0). The linear plot for modified electrodes vs. oxidation peak current as shown in Fig. S8. Further, the sensor has a good reproducibility with a relative standard deviation (RSD) of 3.2% for 5 individual analysis performed at 5 modified electrodes which were prepared.

To investigate the long-term storage stability under the desired condition was also tested for 60 days. The current response of the sensor decreases to 97.45%, 97.12%, 96.45%, and 94.87% of the original response after a month, might be due to the depletion of dissolved oxygen. These findings prove the good storage stability, which is most likely due to the strong interaction between reduced graphene oxide and carbon black material. These results showed that prepared electrode had high selectivity, ideal reproducibility, and excellent long-term storage stability in the electrochemical detection of CA.

Analytical applicability

To evaluate the practical ability of the Chit-CB/rGO/GCE nanocomposites, the fabricated electrode was also used for the estimation of CA in wine samples using DPV method

Table 1 Comparison of composition and performance of electrodes used for determination of CA

[a]Electrode	Method	LDR (μmol/L)	LOD (μmol/L)	Ref.
$CoFeSe_2$/f-CNF/GCE	DPV	0.01–263.96	0.20×10^{-9}	[28]
Au/PdNPs-GRF	DPV	0.03–938.97	0.60×10^{-9}	[29]
NDC/GCE	DPV	0.01–350	0.24×10^{-9}	[30]
AuNPs/GRNS	DPV	0.5–50	5.00×10^{-8}	[31]
ERGO/SPCE	SWV	0.2–2100	0.64×10^{-8}	[32]
Au-PEDOT/rGO/GCE	DPV	01–46	0.40×10^{-9}	[33]
Au-PdNPs/GRF/GCE	DPV	0.03–938.97	0.60×10^{-9}	[34]
Pt-PEDOT/rGO/GCE	DPV	$5.0 \times 10^{-9} – 4.0 \times 10^{-6}$	$2\ 10 \times 10^{-9}$	[35]
AuNPs/rGO/GCE	DPV	0.5–5	0.50×10^{-7}	[36]
PG films/GCE	SWV	$4.0 \times 10^{-6} – 3.0 \times 10^{-5}$	1.25×10^{-6}	[37]
p-NPDS/GCE	CV	0.1–22	0.10×10^{-7}	[38]
Au@α-Fe_2O_3[f]@RGO@GCE	DPV	19–1869	0.98×10^{-6}	[39]
Chemically reduced graphene oxide	AMP	$1.0 \times 10^{-8} – 8.0 \times 10^{-4}$	0.20×10^{-9}	[40]
MnO_2/CM/GCE	SWV	1.00–15.00	2.70×10^{-7}	[41]
Chit-CB/rGO/GCE	DPV AMP	0.6×10^{-6}-10.6×10^{-5} 0.6×10^{-9}-57.3×10^{-5}	0.021×10^{-6} 0.03×10^{-9}	[This work]

f-CNF- Carbon Nanofibre

Au/PdNPs-GRF - Gold/Palladium nanoparticles-Graphene

NDC/G – Nitrogen doped Carbon

AuNPs/GRNS - Gold nanoparticles/graphene nanosheets

ERGO – Electrochemical reduction of graphene oxide

GRF – graphene flakes

PEDOT – Polyethylenedioxythiphene

PG films/GCE – Poly glutamic acid films

p-NPDS – p-nitrophenyl diazonium salt,

CM – Carbon micrporous

[45]. All analytical experiments, 30 mL wine samples were taken and then made up to 100 mL standard flask utilizing doubly distilled water and 50 μL of this solution was taken from the stock solution and then injected into the buffer (15 mL). An aliquot of 15 mL of this solution was kept in the electrochemical cell and certain amount of 10 mM CA was spiked utilizing the standard method. The analytical outputs are shown in Table 2. The recovery range of CA is 99.0–103.0% and RSD was noted to be < 5%. This accurate result was further confirmed by comparing with the output found by HPLC. The present analysis is attested well and complements the earlier literature have been studied with high-performance analyses [42]. Hence, the current method might be considered as right and suitable for the determination of CA in wine beverages.

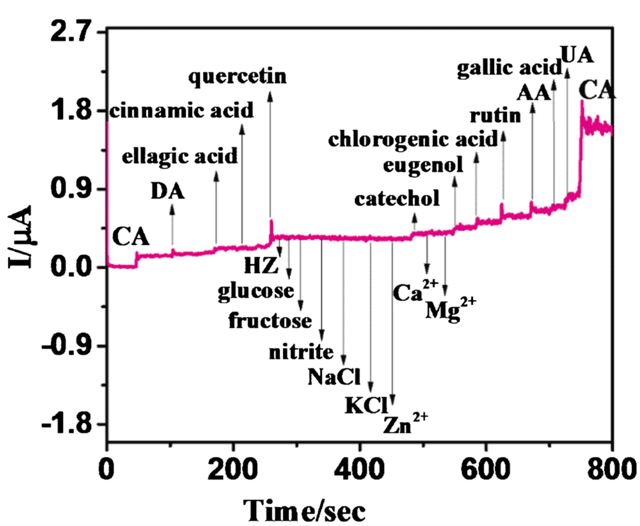

Fig. 5 Amperomertic response of adding different interfering compounds at Chit-CB/rGO modified GCE in the occurrence of 0.1 μM of caffeic acid via 0.1 M buffer (pH 3.0)

Conclusion

The present work demonstrated that the electrode modification of a glassy carbon electrode with carbon materials (CB/rGO) within a chitosan film permits good enhancements for the diagnosis of caffeic acid at pH 3.0. The nanohybrid composite layer of modified electrode enhanced electrochemical current signal with excellent stability which facilitates the electrochemical oxidation of CA at lower over potential

Table 2 Detection of CA in different wine samples *(n = 4)*

Sample	Added (μM)	Found (μM)	R.S.D. (%)	Recovery (%)	Amount found by HPLC method
Red wine	50	49.9 ± 2.4	4.6	99.8	48.6 ± 2.0
	70	71.3 ± 2.0	2.9	101.8	69.0 ± 1.4
	90	90.8 ± 1.4	1.5	100.9	90.3 ± 3.2
White wine	50	49.5 ± 1.8	3.7	99.0	50.6 ± 0.7
	70	72.3 ± 1.4	2.0	103.0	70.2 ± 2.5
	90	91.6 ± 3.2	3.5	101.7	91.9 ± 2.6
Pink wine	50	49.0 ± 1.7	3.3	98.0	50.9 ± 0.9
	70	70.5 ± 2.0	2.9	100.7	70.0 ± 3.1
	90	91.6 ± 1.9	2.0	101.7	89.0 ± 1.6

ranges. Based on the improved electrochemical response the current system can be used for the voltammetry analysis of CA in wine and beverages. For the quantitative detection of CA and to measure the unknown concentrations of CA the standard addition method was employed. This method also used to quality and to determine the shelf life of wine and beverages products. Electrochemical results proved that a low detection limit with a wide concentration ranges calibration plot and excellent sensitivity of the modified electrode system.

Acknowledgements Prof. K.P. thanks Prof. M.V. Sankaranarayanan and Mrs. M. V. Beena, Department of Chemistry, IIT Madras; Chennai for permitting to use the laboratory facility for electrochemical instrument studies (EIS). We thank Dr. M. Saroja devi, Department of chemistry, Anna University for giving FT-IR facility. The authors also thank the DST-PURSE, New Delhi, and the University of Madras for permitting us to avail AFM facility.

Compliance with ethical standards The author(s) declare that they have no competing interests.

Publisher's Note Springer Nature remains neutral with regard to jurisdictional claims in published maps and institutional affiliations.

References

1. Erk T, Hauser J, Williamson G, Renouf M, Steiling H, Dionosi F, Richling E (2014) Structure and dose-absorption relationships of coffee polyphenols. Biofactors 40:103–112. https://doi.org/10.1002/biof.1101
2. Veljkovic JN, Pavlovic AN, Mitic SS, Tosic SB, Stojanovic GS, Kalicanin BM, Stankovic DM, Stojkovic MB, Mitic MN, Brcanovic M (2013) Evaluation of individual phenolic compounds and antioxidant properties of black, green, herbal and fruit tea infusions consumed in Serbia: spectrophotomaterial and electrochemical approaches. J. Food. Nutr Res 52:12–24
3. Sousa WR, Rocha CD, Cardoso CL, Silva DHS, Zanoni MVB (2004) Determination of the relative contribution of phenolic antioxidants in orange juice by voltammetric methods. J Food Composition Anal 17:619–633. https://doi.org/10.1016/j.jfca.2003.09.013
4. Rebelo MJ, Rego R, Ferreira M, Oliveira MC (2013) Comparative study of the antioxidant capacity and polyphenol content of Douro wines by chemical and electrochemical methods. Food Chem 141:566–573. https://doi.org/10.1016/j.foodchem.2013.02.120
5. Leite FRF, Santos WDJR, Kubota LT (2014) Selective determination of caffeic acid in wines with electrochemical sensor based on molecularly imprinted siloxanes. Sens Actuators B: Chem 193:238–246. https://doi.org/10.1016/j.snb.2013.11.028
6. Weng CJ, Yen GC (2012) Chemopreventive effects of dietary phytochemicals against cancer invasion and metastasis: phenolic acids, monophenol, polyphenol, and their derivatives. Cancer Treat Rev 38:76–87. https://doi.org/10.1016/j.ctrv.2011.03.001
7. Prasad NR, Karthikeyan A, Karthikeyan S, Reddy BV (2011) Inhibitory effect of caffeic acid on cancer cell proliferation by oxidative mechanism in human HT-1080 fibrosarcoma cell line. Mol Cell Biochem 349:11–19. https://doi.org/10.1007/s11010-010-0655-7
8. Ikeda K, Tsujimoto K, Uozaki M, Nishide M, Suzuki Y, Koyama AH, Yaasaki H (2011) Inhibition of multiplication of herpes simplex virus by caffeic acid. Int J Mol Med 28:595–598. https://doi.org/10.3892/ijmm.2011.739
9. Peng Y, Liu F, Ye J (2005) Determination of phenolic acids and flavones in Lonicera japonica thumb by capillary electrophoresis with electrochemical detection. Electroanalysis 17:356–362. https://doi.org/10.1002/elan.200403102
10. Carrasco A, Ortiz-Ruiz, Martinea-Gutierrez R, Tomas V, Tudela J (2015) Lavandulastoechas essential oil from Spain: Aromatic profile determined by gas chromatography-mass spectrometry, antioxidant and lipoxygenase inhibitory bioactivities, Ind Crop Prod 73:16–27. https://doi.org/10.1016/j.indcrop.2015.03.088.
11. Wang X, Wang J, Yang N (2006) Flow injection chemiluminescence detection of gallic acid in olive fruits. Food Chem 105:340–345. https://doi.org/10.1016/j.foodchem.2006.11.061
12. Daniela PS, Marcio FB, Amold GF, Maria VBZ (2005) Application of a glassy carbon electrode modified with poly(glutamic acid) in Caffeic acid determination. Microchim Acta 151:127–134. https://doi.org/10.1007/s00604-005-0374-z
13. Mao JS, Liu HF, Yin YJ, Yao KD (2003) The properties of chitosan-gelatin membranes and scaffolds modified with hyaluronic acid by different methods. Biomaterials 24:1621–1629. https://doi.org/10.1016/S0142-9612(02)00549-5
14. Sato T, Ishii T, Okahata Y (2001) In vitro gene delivery mediated by chitosan. Effect of pH, serum, and molecular mass of chitosan on the transfection efficiency. Biomaterials 22:2075–2080. https://doi.org/10.1016/S0142-9612(00)00385-9
15. Zappino M, Cacciotti I, Benucci I, Nanni F, Liburdi K, Valentini F, Esti M (2015) Bromelain immobilization on microbial and animal source chitosan film for application in wine-like medium:

microstructural, mechanical, and catalytic characterizations. Food Hydrocoll 45:41–47. https://doi.org/10.1016/j.foodhyd.2014.11.001
16. Gingras M, Paradis I, Berthod F (2003) Nerve regeneration in a collagen-chitosan tissue-engineered skin transplanted on nude mice. Biomaterials 24:1653–1661. https://doi.org/10.1016/S0142-9612(02)00572-0
17. Yang X, Tu Y, Li L, Shang S, Tao XM (2010) Well-dispersed chitosan/graphene oxide nanocomposites. Appl Mater Interface 2: 1707–1713. https://doi.org/10.1021/am100222m
18. Talarico D, Arduini F, Amine A, Cacciotti I, Moscone D, Palleschi G (2016) Screen-printed electrode modified with carbon black and chitosan: a novel platform for acetylcholinesterase biosensor development. Anal Bioanal Chem 408:7299–7309. https://doi.org/10.1007/s00216-016-9604-y
19. Shao Y, Wang J, Wu H, Liu J, Aksay IA, Lin Y (2010) Graphene based electrochemical sensors and biosensors: a review. Electroanalysiss 22:1027–1036. https://doi.org/10.1002/elan.200900571
20. Vilian AT, Chen SM, Chen YH, Ali MA, Al-Hemaid (2014) An electrocatalytic oxidation and voltammetric method using a chemically reduced graphene oxide film for the determination of caffeic acid. J. Colloids Interface Sci. 423: 33–40. https://doi.org/10.1016/j.jcis.2014.02.016.
21. Wang N, Lin M, Dai H, Ma H (2016) Functionalized gold nanoparticles/reduced graphene oxide nanocomposites for ultrasensitive electrochemical sensing of mercury ions based on thymine-mercury-thymine structure. Biosens Bioelectron 79:20–326. https://doi.org/10.1016/j.bios.2015.12.056
22. Qin W, Li D, Zhang X, Yan D, Hu B, Pan L (2016) ZnS nanoparticles embedded in reduced graphene oxide as high-performance anode material of sodium ion batteries. Electrochim Acta 191: 435–443. https://doi.org/10.1016/j.electacta.2016.01.116
23. Marina B, Santos FS, Vicentini FC, Zucolotto V, Janegitz BC, Filho OF (2017) Electrochemical sensor based on reduced graphene oxide/carbon black /chitosan composite for the simultaneous determination of dopamine and paracetamol concentrations in urine samples. J Electroanal Chem 799:439–443. https://doi.org/10.1016/j.jelechem.2017.06.052
24. Song L, Khoerunnisa F, Gao W, Dou W, Hayashi T, Katsumi K, Enda M, Ajayan PM (2013) Effect of high-temperature thermal treatment on the structure and adsorption properties of reduced graphene oxide. Carbon 52:605–620. https://doi.org/10.1016/j.carbon.2012.09.060
25. Nethravathi C, Rajamathi M (2008) Chemically modified graphene sheets produced by the solvothermal reduction of colloidal dispersions of graphite oxide. Carbon 46:1994–1998. https://doi.org/10.1016/j.carbon.2008.08.013
26. Alwarappam S, Cissell K, Dixit S, Li CZ, Mohapatra S (2012) Chitosan-modified graphene electrodes for DNA mutation analysis. J Electroanal Chem 686:69–72. https://doi.org/10.1016/j.jelechem.2012.09.026
27. Kalaiyarsi J, Meenakshi S, Pandian K, Gopinath SCB (2017) Simultaneous voltammetric determination of vanillin and guaiacol in food products on defect free graphene nanoflake modified glassy carbon electrode. Microchim Acta 184:2131–2140. https://doi.org/10.1007/s00604-017-2161-z
28. Mani S, Sukanya R, Shen MC, Bose D, Hari VR, Lee YS (2018) Entrapment of bimetallic $CoFeSe_2$ nanosphere on functionalized carbon nanofiber for selective and sensitive electrochemical detection of caffeic acid in wine samples. Anal Chim Acta 1006:22–32. https://doi.org/10.1016/j.aca.2017.12.044
29. Kokulnathan T, Raja N, Chen SM, Liao WC (2017) Nanomolar electrochemical detection of caffeic acid in fortified wine samples based on gold/palladium nanoparticles decorated graphene flakes. J Colloid Interface Sci 501:77–85. https://doi.org/10.1016/j.jcis.2017.04.042
30. Karikalan N, Karthick R, Chen SM, Chen HA (2017) A voltmmetric determination of caffeic acid in red wines based on the nitrogen doped carbon modified glassy carbon electrode. Sci Rep 7:45924. https://doi.org/10.1038/srep45924
31. Zhang Y, Liu Y, He J, Pang Y, Gao Y, Hu Q (2013) Electrochemical behaviour of caffeic acid assayed with gold nanoparticles/grapheme nanosheets modified glassy carbon electrode. Electroanalysis 25: 1230–1236. https://doi.org/10.1002/elan.201200587
32. Velmurugan M, Balasubramanian P, Chen SM (2017) Determination of Caffeic acid in wine samples based on the electrochemical reduction of graphene oxide modified screen printed carbon electrode. Int J Electrochem Sci 12:4173–4182. https://doi.org/10.20964/2017.05.01
33. Liu Z, Xu J, Yue R, Yang T, Gao L (2016) Facile one-pot synthesis of Au-PEDOT/rGO/GCE nanocomposite for highly sensitive detection of caffeic acid in red wine sample. Electrochim Acta 196:1–12. https://doi.org/10.1016/j.electacta.2016.02.178
34. Thangavelu K, Raja N, Chen SM, Liao WC (2017) Nanomolar electrochemical detection of caffeic acid in fortified wine samples based on gold/palladium nanoparticles decorated graphene flakes. J Colloid Interface Sci 501:2971–2981. https://doi.org/10.1016/j.jcis.2017.04.042
35. Lei G, Ruirui Y, Jingkun X, Zhen L, Jingdang C (2018) Pt-PEDOT/rGO nanocomposites: one-pot preparation and superior electrochemical sensing performance for caffeic acid in tea. J Electroanal Chem 816:14–20. https://doi.org/10.1016/j.jelechem.2018.03.024
36. Zhang Y, Liu Y, He J, Pang P, Gao Y, Hu Q (2013) Electrochemical behaviour of caffeic acid assayed with gold nanoparticles/graphene nanosheets modified glassy carbon electrode. Electroanalysis 25: 1230–1236. https://doi.org/10.1002/elan.201200587
37. Santos PD, Bergamini MF, Fogg AG, Zanoni MVB (2005) Application of a glassy carbon electrode modified with poly(glutamic acid) in Caffeic acid determination. Microchim Acta 151:127–134. https://doi.org/10.1007/s00604-005-0374-z
38. Pulg MC, Berbel XM, Blanchard CC, Marty JL (2010) Diazonium-functionalized tyrosinase-based biosensor for the detection of tea polyphenols. Microchimi Acta 171:187–193. https://doi.org/10.1007/s00604-010-0425-y
39. Bharath G, Alhseinat E, Madhu R, Mugo SM, Alwasel S, Harrath AH (2018) Facile synthesis of au@α-Fe_2O_3@RGO ternary nanocomposites for enhanced electrochemical sensing of caffeic acid toward biomedical applications. J Alloys compounds 750:819–827. https://doi.org/10.1016/j.jallcom.2018.04.052
40. Vilian EAT, Chen SM, Chen YH, Ali MA, Al-Hemaid FMA (2014) An electrocatalytic oxidation and voltammetric method using a chemically reduced graphene oxide film for the determination of caffeic acid. J Colloid Interface Sci 423:33–40. https://doi.org/10.1016/j.jcis.2014.02.016
41. Li J, Jiang J, Liu M, Xu Z, Deng P, Qian D, Tong C, Xie H, Yang C (2017) Facile synthesis of MnO_2-embedded flower-like hierarchical porous carbon microspheres as an enhanced electrocatalyst for sensitive detection of caffeic acid. Anal Chim Acta 985:155–165. https://doi.org/10.1016/j.aca.2017.07.002
42. Seruga M, Novak I, Jakobek L (2011) Determination of polyphenols content and antioxidant activity of some red wines by differential pulse voltammetry, HPLC and spectrophotometric methods. Food Chem 124:1208–1216. https://doi.org/10.1016/j.foodchem.2010.07.047